

# RSC Advances



This is an *Accepted Manuscript*, which has been through the Royal Society of Chemistry peer review process and has been accepted for publication.

*Accepted Manuscripts* are published online shortly after acceptance, before technical editing, formatting and proof reading. Using this free service, authors can make their results available to the community, in citable form, before we publish the edited article. This *Accepted Manuscript* will be replaced by the edited, formatted and paginated article as soon as this is available.

You can find more information about *Accepted Manuscripts* in the [Information for Authors](#).

Please note that technical editing may introduce minor changes to the text and/or graphics, which may alter content. The journal's standard [Terms & Conditions](#) and the [Ethical guidelines](#) still apply. In no event shall the Royal Society of Chemistry be held responsible for any errors or omissions in this *Accepted Manuscript* or any consequences arising from the use of any information it contains.

**Morphological evolution and toughening mechanism  
of Polypropylene and Polypropylene/ poly  
(ethylene-co-octene) alternating multilayered  
materials with enhanced low temperature toughness**

Jianfeng Wang, Cuilin Wang, Xianlong Zhang, Hong Wu\*, Shaoyun Guo\*

*The State Key Laboratory of Polymer Materials Engineering, Polymer Research*

*Institute of Sichuan University, Chengdu 610065, China*

**ABSTRACT**

In this paper, polypropylene (PP) and polypropylene/poly (ethylene-co-octene) blends (PP/POE) were fabricated into alternating multilayered materials to improve the low temperature toughness of PP efficiently, compared with conventional PP/POE blends. POM, SEM, Micro-FTIR and part-impact test were performed to characterize and investigate the alternating multilayered microstructure and its relationship with mechanical properties. The results showed that the unique alternating multilayered microstructure could generate distinctive distribution of POE, resulting in the great change of both macro and micro-morphology of the materials. Most interestingly, the morphological evolution of the dispersed POE phase before and after the impact showed that a brittle-ductile transition (BDT) layer was formed at the interlayer interface between adjacent PP layer and PP/POE layer during the impact

---

\* To whom correspondence should be addresses. (Prof. Wu, Email: [wh@scu.edu.cn](mailto:wh@scu.edu.cn), Fax: 86-028-85466077)

\* To whom correspondence should be addresses. (Prof. Guo, Email: [sguo@scu.edu.cn](mailto:sguo@scu.edu.cn), Fax: 86-028-85405135)

process, which was the main reason for the great improvement of low temperature toughness. Moreover, the rigidity of alternating multilayered materials was kept very well due to the existence of the rigid PP layer, indicating that alternating multilayered microstructure was very helpful to keep a good balance between toughness and rigidity.

**Keywords:** Alternating multilayered microstructure; Low temperature toughness; PP; Morphological evolution; Toughening mechanism

## INTRODUCTION

Polymer toughening is one of general and important topics in the research of polymer material science because the applications of many polymers are greatly restricted due to their poor toughness. And polymer blending has always been considered as a simple and feasible way to improve the toughness of the polymers. At the earliest, the elastomers were extensively used as toughening agents due to their excellent elasticity and toughness. It is well-known that many factors have influence on the toughening effect, such as the properties of matrix [1, 2], the structure of polymer blends [3-6], the interfacial adhesion and compatibility between the matrix and elastomer fillers [7, 8], shape [9], size [9-11] and distribution [12] of elastomer particles in the matrix. Moreover, in order to obtain material with greatly improved toughness, especially at low temperature, large amounts of the elastomer must be

added into the polymer [13]. However, the rigidity of the material is sacrificed seriously due to the low modulus of the elastomer and the cost is increased due to the expensive price of the elastomer. To overcome the drawbacks resulted by adding elastomer, some studies [14-18] have been done on polymer/elastomer/rigid filler ternary system. It has been found that the dispersed phase morphology and microstructure of ternary blends is very important for achieving the best combination of mechanical properties.

Therefore, many studies [19-22] have already been focused on how to achieve material with balanced toughness and rigidity by adjusting dispersed phase morphology and microstructure of the toughening system. Hongjun Xu et al [23] regulated phase morphology and microstructure of PP material successfully through the photocrosslinking under UV radiation, and both its toughness and tensile strength were enhanced simultaneously due to more rigid mSEBS dispersed phase and strong interfacial bonding between the mSEBS dispersed phase and the PP matrix. Hong Yang et al. [24] achieved a core-shell structure, where EPDM particles were closely surrounded with hydrophilic SiO<sub>2</sub> particles in the PP matrix, through two-step processing. The results showed that the toughness and the modulus of PP were enhanced simultaneously due to the overlap of the 'stress volume' between EPDM and SiO<sub>2</sub> particles caused by the unique microstructure above. Nonetheless, the attentions of

most studies were paid to the influence of the microstructure and morphology on the performance of the materials. To the best of our knowledge, the effect of impact process on the evolution of the microstructure and morphology was hardly reported, in spite of its importance to understand the toughening mechanism profoundly.

It is well-known that polypropylene (PP), as one of important commodity plastics, has been widely used in construction industry, automobile and household appliance. However, the application of PP is limited greatly by its low impact strength, especially at low temperature below  $T_g$ , as well as poor rigidity at elevated temperature. Therefore, a lot of studies [13, 18, 20, 22, 23, 24] have been done to achieve the PP with balanced toughness and rigidity. Some recent work of Zhigang Wang [25-27] found that the layer-by-layer method can generate new polymer materials with much improved morphologies and physical properties as compared with the regular blends. Moreover, Mohit Gupta et al [28] successfully fabricated alternating poly(propylene-graft-maleic) (PP-g-MA) and poly(propylene-graft-maleic)/phosphate glass (PP-g-MA/Pgalss) multilayered film with reduction in gas permeation by two to three orders of magnitude compared with the neat PP-g-MA. More interestingly, the modulus of the alternating multilayered film was increased effectively without any considerable loss in ductility. However, the reason for the as-obtained balanced mechanical performance was not

discussed in detail. In our opinions, it should be ascribed to the existence of multilayered microstructure alternating with relatively ductile PP-g-MA and rigid PP-g-MA/Pglass. And the ductile PP-g-MA layer and rigid PP-g-MA/Pglass layer can support each other in the mechanical tests.

In the present work, we try to introduce the alternating multilayered microstructure into PP toughening system by alternating PP matrix with another ductile PP/POE blends layer through multilayered co-extrusion technology, which was developed in our lab. The stratified composite sheets are prepared with alternating polymer layers, where each layer is continuous along the extrusion direction [29]. Alternating multilayered materials with unique macro and micro-morphologies will be investigated comparatively with conventional blends. Our main goal is to fabricate PP with enhanced low temperature toughness and balanced rigidity at evaluated temperature. In addition, the relationship between microstructure and properties will be discussed, for the first time as far as we known, by investigating the morphological evolution of dispersed POE phase during the impact process. It will provide not only a deep understanding in the toughening mechanism but also a new approach for obtaining PP with balanced mechanical properties.

## **2 EXPERIMENTAL**

### **2.1 Materials**

The PP was 1300 with a MFI of 2.5 g/10 min at 215 °C, 2.16 Kg, supplied by Mao Ming Petro-chemistry Co. The POE was Engage 8150 manufactured by Du Pont-Dow Chemical, with an octane content of 25% and a MFI of 0.8 g/10min, at 215 °C, 2.16 Kg. Their densities were  $0.909 \times 10^3$  and  $0.863 \times 10^3$  kg/m<sup>3</sup>, respectively.

## 2.2 Sample preparation

Firstly, PP and PP/POE blends with varied weight ratios (90/10, 80/20 and 70/30) were extruded through a twin-screw extruder. The temperature of mixing section was 170-190-200-200-195°C from the hopper to the die, and then the blends were dried in the vacuum drying chamber for 24 h after being cut with the granulator. The MFI of PP/POE blends with 0, 10, 20, 30 wt% POE, tested at 215 °C, 2.16 Kg, are 2.5, 2.3, 2.0, 1.7 g/10min, respectively. Then, PP and PP/POE blends were coextruded as alternative multilayered materials using multilayered co-extrusion technology, and the temperature settings of the extruders for PP section and PP/POE blends section were 160-200-215-215-210°C and 90-200-215-215-210°C, respectively. The sketch of the co-extrusion technology was illustrated in Fig.1. PP/POE blends and neat PP were extruded simultaneously from different extruders, and merged into 2-layer melt in the co-extrusion block, and then the melt flowed through a series of layer multiplying elements (LMEs). In a LME, the melt was sliced into two left and right sections by a divider, and then recombined

vertically as shown in Fig. 1. An assembly of  $n$  LMEs could produce the alternating multilayered material with  $2^{(n+1)}$  layers.

In this study, alternating multilayered samples with 128 layers were extruded by using 6 LMEs. The overall sheet thickness ranged from 1700  $\mu\text{m}$  to 1800  $\mu\text{m}$ . The nominal PP layer and PP/POE layer thickness was calculated from the number of layers, the sheet thickness and the total POE content. The total POE content can be changed by adjusting the extruder speed of PP/POE section and the composition ratio of PP/POE blends section. Then, the total POE content was calculated from the following formula:

$$W_{\text{POE}} = \frac{(\rho_{\text{PP}} - \rho_{\text{b}}) \times \rho_{\text{POE}}}{\rho_{\text{b}} \times (\rho_{\text{PP}} - \rho_{\text{POE}})} \quad (1)$$

where,  $W_{\text{POE}}$  is the mass fraction of POE ;  $\rho_{\text{b}}$  is the density of the blend;  $\rho_{\text{PP}}$ ,  $\rho_{\text{POE}}$ , represent the densities of neat PP and POE, values of which are  $0.909 \times 10^3$  and  $0.863 \times 10^3 \text{ kg/m}^3$ , respectively. The densities of  $\rho_{\text{b}}$ ,  $\rho_{\text{PP}}$ ,  $\rho_{\text{POE}}$ , were measured through a High precision density tester (MatsuHaku, GH-120M). The as-obtained materials are coded according to the abbreviation for alternating multilayered materials (AM) and the content of POE. For example, AM-18 represents the alternating multilayered material with about 18 wt% POE. Table 1 summarizes the characteristics of these layered samples. For comparison, conventional PP/POE blends and neat PP samples were prepared under the same heat and shearing

force history, using one extruder of multilayered co-extrusion technology with 6 LMEs.

## **2.3 Mechanical properties tests**

### **2.3.1 Notched Izod impact test**

The notched Izod impact strength was tested following GB/1943-2007 with a XJU-22 impact test machine. The sample, whose size was  $80 \times 10 \times 10 \text{ mm}^3$ , was prepared through the compression molding of the alternating multilayered sheets at  $180 \text{ }^\circ\text{C}$ , under 10 MPa. The depth of the notch was 2.0 mm. All the samples were placed in Environmental simulation chambers (Binder, MKFT240) for 15 h at  $-40 \text{ }^\circ\text{C}$ , 40 % relative humidity. Then, samples were taken out quickly for notched Izod impact test through different directions as shown in Fig.2. In order to understand the impact test clearly, we introduced a three-dimensional rectangular coordinate system (as seen in Fig 2): x is the direction of the flow, y is the direction through the layer plane, z is the direction parallel to the layer plane. Each impact test included 5 parallel experiments, and the results were averaged.

### **2.3.2 Tensile yield strength, flexural modulus and strength tests**

Standard tensile test was conducted at room temperature using tensile test machine (model CMT-4104) according to GB/T 1040-92. The dumbbell shaped sample, prepared directly with the sheets extruded by the multilayered co-extrusion technology, was tested through x direction

at a tensile rate of 100 mm/min. The flexural tests were measured according to GB/9341-2000 using the CMT-4104 flexural test machine at room temperature. The sample, whose size was  $80 \times 10 \times 4 \text{ mm}^3$ , was prepared through the compression molding of the alternating multilayered sheets at  $180 \text{ }^\circ\text{C}$ , under 10 M Pa, and then, tested through y direction with a speed of 2 mm/min. At least five parallel specimens were tested in each test.

#### **2.4 Polarized optical microscopy (POM) observation**

Polarized optical microscopy (POM, Leica, DM2500P) was used to assess the layer integrity and continuity. The 20- $\mu\text{m}$  slice sample was cut from the extruded sheet vertical to the flow direction by using a rotary microtome (YD-2508B).

In order to understand the fracture and toughening mechanism of conventional blends and alternating multilayered materials, the crack initiation and propagation stage were observed through a part-impact test, which was performed with the XJU-22 impact test machine. The specimen was also placed in Environmental simulation chambers (Binder, MKFT240) for 15 h at  $-40 \text{ }^\circ\text{C}$ , 40 % relative humidity before the part-impact. The pendulum was raised at an angle of  $60^\circ$  from the vertically fixed specimen, and then released to hit the specimen with appropriately constant impact energy of about 0.5 J. The specimen was not broken into two halves as expected, and the propagating crack or

craze stopped in the interior of the specimen. Similar to the method used to investigate the alternating multilayered microstructure, the initiation and propagation patterns of crack or craze were collected by POM, with the 30- $\mu\text{m}$  sample slices cut from part-impact specimens along the crack propagation direction but perpendicular to the impact direction. The pictures collected by POM were all recorded with a Pixelink camera (PL-A662).

### **2.5 Scanning electron microscopy (SEM)**

Scanning Electron Microscopy (SEM, JSM-5900LV, Japan) were performed to examine the impact fractured surface, the morphological evolution of dispersed POE phase in conventional blends and alternating multilayered materials during the impact process. The samples, used for investigating morphological evolution, were prepared using ultrathin freezing microtome (Leica, RM2265) at  $-100\text{ }^{\circ}\text{C}$ . The as-obtained samples used for investigating morphological evolution were then chemically etched surface of materials with heptane in the oil bath at  $100\text{ }^{\circ}\text{C}$  for 10 h, preferentially dissolving the POE phase.

### **2.6 Micro-FTIR Study**

The molecular orientation of PP and POE along x direction in neat PP, conventional blend and alternating multilayered material were monitored by a Thermo Nicolet infrared microscope, which allows for qualitative assessment of the POE content in alternating multilayered

materials. The IR source was provided by a Thermo Nicolet FTIR spectrometer with a resolution of  $2\text{ cm}^{-1}$  and an accumulation of 32 scans. The test slice sample with thickness of  $30\text{ }\mu\text{m}$  was cut by the rotary microtome (YD-2508B) along x direction directly from the extruded sheet. Polarized infrared spectra, parallel and perpendicular to sampling region, respectively, were collected by rotating a ZnSe polarizer.

The orientation function  $f$ , dichroic ratio  $R$  and structural absorbance  $A$  of a desired absorption band are deduced using the following relations [30]:

$$f = \frac{R - 1}{R + 2} \quad (2)$$

$$R = \frac{A_{\parallel}}{A_{\perp}} \quad (3)$$

Where  $A_{\parallel}$  and  $A_{\perp}$  are the parallel and perpendicular absorbance at the same positions, respectively.

### 3 RESULTS AND DISCUSSION

#### 3.1 Microstructure and morphology analysis

The most difference between alternating multilayered material and conventional blend with the same POE content could be understood reasonably as followed: the dispersed POE phase was layered together through co-extrusion technology to produce a multilayered microstructure alternating with PP layer and PP/POE layer. As expected, this unique multilayered microstructure alternating with PP layer and PP/POE layer

was successfully fabricated, which can be well observed through POM images presented in Fig.3. The macro-anisotropy in the alternating multilayered microstructure is very obviously and the continuity of each layer is very good. This unique microstructure is considered to have a great influence on the toughening system, so investigations from macroscopic perspective and microscopic perspective were conducted in detail later.

The effect of the unique microstructure on the morphology of dispersed POE phase was observed through SEM images of alternating multilayered material (AM-18) and conventional blend (C-20) before the impact. As indicated in Fig.4, the size and deformation of POE particles in AM-18 along both x direction and z direction become much larger than that in C-20. It has been known that the POE content in PP/POE layer in AM-18 and in C-20 are 30 wt% and 20 wt%, respectively. Such a huge difference on POE content is reasonable to be considered as the most important factors affecting the size and deformation of POE particles [13]. Interestingly, the larger deformation of POE particles, resulting from this unique microstructure, would be able to improve the impact strength of the PP matrix when the external force is loaded perpendicular to the direction of deformation [31].

### 3.2 Micro-FTIR analysis

Fig 5 shows the FTIR spectra absorbance of neat PP, neat POE,

conventional blend (C-20), interlayer interface in the PP/POE layer of alternating multilayered material (AM-18) and the PP/POE center layer of AM-18. The vibration absorbance peak at  $720\text{ cm}^{-1}$ , which should be attributed to the bending vibration of side hexyl of POE molecular chain, can be considered as the characteristic absorbance peak of POE. The vibration absorbance peak at  $973\text{ cm}^{-1}$ , due to the contribution of both crystalline and amorphous phase of PP component [30], can be regarded as the characteristic absorbance peak of PP. It is well known that the height and area of the absorption peak is related to the material content positively [32, 33]. As shown in Fig5 and table 2, the absorbance peak height and area at  $720\text{ cm}^{-1}$  of POE in the interlayer of AM-18 is stronger than that in C-20, but weaker than that in the center of PP/POE layer of AM-18. The peak area ratio between  $720\text{ cm}^{-1}$  and  $973\text{ cm}^{-1}$  of the same sample, which can eliminate the effect of the sample thickness and qualitatively assess the difference of POE content, presents the similar trend with the peak height and area. This is attributed to the existence of each PP/POE layer in the alternating multilayered microstructure, which can be regarded as a micro-pipe compared with conventional blend. Radical migration [34] of dispersed deformable POE particles would take place in each PP/POE layer, resulting in stratification of POE content in PP/POE layer. The POE content in the center of PP/POE layer in AM-18 becomes higher than 30 wt% and that at the interlayer interface between

PP layer and PP/POE layer becomes lower than 30 wt%. Therefore, the interlayer interface between the adjacent layers can be regarded as a transition layer, due to the stratification of POE content.

Moreover, the viscosity of PP/POE blends increases with increasing POE content. Stratification of viscosity will take place in the alternating multilayered microstructure, due to the stratification of POE content. And the stratification of viscosity is considered to generate great influence on the PP molecules and POE molecules during the processing process. So the orientation of PP molecules and POE molecules along x direction in AM-18 were monitored through the Micro-FTIR study, compared with that in neat PP and C-20. To determine the orientation function of PP and POE, some characteristic bands were examined. As shown in Fig6, the  $973\text{ cm}^{-1}$  vibration is usually used to evaluate both crystalline and amorphous phases of PP, namely the average orientation function (f) [30]. The  $720\text{ cm}^{-1}$  vibration is used to estimate the orientation function of POE, according to the FTIR of neat POE. As shown in table 2, the orientation function of PP molecules and POE molecules in AM-18 present a gradient distribution phenomenon, reducing gradually from PP layer to the transition layer and PP/POE layer. This is consistent with the stratification of POE content. Moreover, the orientation function of PP molecules and POE molecules in PP/POE layer in AM-18 decreased compared with that in conventional blend. This also indicates that the

difference of POE content have a great influence on the PP molecules and POE molecules.

Combining the above results, one can observe that the unique alternating multilayered microstructure can generate distinctive distribution of POE compared with conventional blends. This distinctive distribution of POE can make great change on both macro and micro-morphology of the blends, which would have a great effect on the performance of material.

### **3.3 Toughness and rigidity**

As indicated in Fig.7 (a)-(d), the mechanical properties of alternating multilayered materials effectively improved compared with that of conventional blends, which just as we had expected. The notched Izod impact strength of alternating multilayered materials and conventional blends at  $-40\text{ }^{\circ}\text{C}$  through different directions all increase with increasing the POE content (seen in Fig.7 (a)). It is interesting that brittle-ductile transition (BDT) of alternating multilayered materials through y direction occurs with about 15 wt% POE, while the conventional blends are still brittle under the same condition. The impact strength of alternating multilayered material is considerably improved when the POE content is only 18 wt%, the value of which increases to  $5.61\text{ KJ/m}^2$ . While the impact strength of the conventional blends with 20 wt% and 30 wt% POE were  $3.71\text{ KJ/m}^2$  and  $6.62\text{ KJ/m}^2$ , respectively. However, nearly no

difference of the impact strength through z direction between alternating multilayered materials and conventional blends can be found, indicating that there is anisotropy on the impact strength of alternating multilayered materials through different directions. On the other hand, the difference of tensile yield strength between alternating multilayered materials and conventional blends was also little, as shown in Fig.7 (b). But the flexural modulus and flexural strength of alternating multilayered materials improve greatly in contrast to that of conventional blends, as shown in Fig.7 (c) and Fig.7 (d). The direction of the external force in tensile tests is along x direction while that in flexural tests is along y direction, which result in the difference between tensile properties and flexural properties. It consists with the difference on impact strength through different directions.

Although the toughness and rigidity through z direction of alternating multilayered materials are hardly enhanced, the toughness and rigidity through y direction are greatly enhanced simultaneously. Now it is therefore logical to ask what leads to the improvement of the toughness and rigidity simultaneously and what is the relationship between microstructure and properties? So the fracture mechanism and toughening mechanism will be discussed in detail later.

### **3.4 Fracture and toughening mechanism**

In order to ascertain the difference in fracture and toughening

mechanism between conventional blends and alternating multilayered materials, the initiation and propagation patterns of crack and craze produced through part-impact test were studied, as presented in Fig.8. Under almost the same impact speed and impact energy, the fracture degree and mechanism of these samples were entirely different. For alternating multilayered material impacted through y direction (AM-18(y)), there had no crack but a big yield-region (dark zone) formed during the part-impact, compared with the existence of obvious crack in alternating multilayered materials impacted through z direction (AM-18 (y)) as well as conventional blends impacted through both y and z direction (C-20 (y) and C-20(z)). In addition, there was almost no difference on the crack initiation and propagation of AM-18 (z), C-20(y) and C-20(z). In the above three samples, massive crazing around the crack tip was initiated and then propagated along the impact direction, and a fan-shaped craze zone was formed around the crack tip. At the same time, massive crazing was also initiated around the yield-region tip in AM-18 (y), but when the craze in PP layer came across PP/POE layer, the stress will be dispersed quickly at the transition layer along the direction parallel to the layer. So the craze in AM-18 (y) propagated not only along the impact direction but also along the direction at a small angle from the layer, thus a rectangle craze zone was formed around the yield-region tip. Moreover, this special type of craze propagation, which was along the

direction at a small angle from the layer, can absorb much impact energy and then prevent the development of craze into crack along the impact direction. The different phenomenon observed between conventional blends and alternating multilayered materials through part-impact was well consistent with the result of notched Izod impact strength.

Furthermore, to gain more insight in understanding the fracture mechanism and toughening mechanism, it is important to investigate the impact fracture surface and morphological evolution of dispersed POE phase in conventional blend and alternating multilayered material during the impact process through different directions. As shown in Fig.9 as well as Fig.10, (a) and (b), (d) and (e) were the two impact fracture surfaces of the same sample, respectively, and the distance of A, B and C away from the notch were 0, 3000 and 6000 $\mu\text{m}$ , respectively. For alternating multilayered material (AM-18) impacted through z direction (Fig 10(e)) and conventional blend (C-20) impacted through y and z directions (as seen in Fig 9(a) and Fig 9(e)), only the impact fracture surfaces near the notch are relatively rough, and the impact fracture surfaces of the three samples above become more and more smooth as the distance away from the notch increases, and the materials break by brittle fracture as a whole. However, all the impact fracture surfaces of alternating multilayered material (AM-18) impacted through y direction are very rough, which are characterizations of tough fracture (seen in Fig 10(a)). What is more, for

C-20 impacted through both y and z directions, the size and deformation of POE particles decrease compared with those before the impact (seen in Fig9(b), Fig9(d) and Fig9(c)). It has been known that dispersed POE particles can initiate crazes and shear band in blends as stress concentration factors [35], and then absorb impact energy to block the propagation of crack. Moreover, the crazes can be terminated when the front end of the craze encounter another POE particles, avoiding the further development of crazes into cracks and thereby improve the toughness of material. Therefore, the morphological evolution of the POE particles during the impact process is a process of impact energy absorption in fact. Besides, the notch plays the role of strain concentrator and takes on most of the strain loading during the impact process [36]. Once the crack is initiated, the stress concentration will increase sharply due to the width of the crack tip is much less than that of the notch tip, which makes the POE particles near the notch absorb much more energy to alleviate the stress concentrated on the cracks and thereby prevent the further development of cracks. However, the farther the fracture area is away from the notch tip, the lower the impact speed is, the less the energy absorbed by POE particles is, and the smaller the change of POE particles is. With regard to AM-18 (seen in Fig10(b), Fig10(d) and Fig10(c)), the size and deformation of POE particles through both y and z directions decrease compared with those before the impact, which are similar with

those of conventional blends. However, due to the unique alternating multilayered microstructure, an interesting phenomenon appears about the dispersed morphology of POE phase in the transition layer between adjacent layers: the size and deformation of POE particles in PP/POE layer are relatively uniform before the impact both in the center of PP/POE layer and in the transition layer, but during the impact, the size of POE particles in the transition layer become smaller than those in the center of PP/POE layer. Besides, it has been known that the conventional blend with 30 wt% POE is ductile and that with 20 wt% is brittle. Therefore, multilayered microstructure alternating with brittle PP layer and ductile PP/POE layer occurs in alternating multilayered materials with 30 wt% POE in the PP/POE layer. Therefore, the transition layer, formed between PP layer and PP/POE layer in the alternating multilayered materials, would play the role of brittle-ductile transition (BDT) layer during the impact process.

However, the formations of the BDT layer through y and z directions are very different. In the case of alternating multilayered material impacted through y direction, the force propagates perpendicular to layers. When the force propagates from the brittle PP layer to the transition layer, the POE particles in the transition layer become stress concentrator quickly to absorb impact energy, then, the particles size decrease dramatically compared with those before the impact. However, the

number of stress concentrator in the center of PP/POE layer became larger than that in the transition layer resulting from the stratification of POE content, and the total energy absorbed by the POE particles in the center of PP/POE layer decreased after the impact energy was absorbed by POE particles in the transition layer. These two factors result in the particles size in this area changing less than that in the transition layer. What is more, when the force propagates from the ductile layer to the brittle layer, a response will be produced on the POE particles in the transition layer to concentrate more stress than that of POE particles in the center of PP/POE layer, due to the difference of POE content. So it can successfully realize the transition from ductile layer to brittle layer, the particles size thereby become smaller than that in the center of PP/POE layer. Therefore, a BDT layer like a bridge connecting the brittle layer and ductile layer is formed in the transition layer during the impact process. However, for alternating multilayered material impacted through z direction, the force propagates along rigid layer and ductile layer, respectively. The POE particles in the transition layer concentrated much more stress than that in the PP/POE center, due to the stratification phenomenon of POE content. Therefore, POE particles in the transition layer absorb more energy than those in the center of PP/POE layer to resist the external force, leading to the particles size at the layer interface become smaller than that in the center of PP/POE layer. And a BDT layer

was also formed in the transition layer during the impact process of AM-18(z).

Most importantly, the impact direction plays a key role in determining the ultimate properties of material. As shown in Fig.11 (a), when the force is loaded perpendicular to the layer, the force can propagate through an alternating circulation in the fracture process: brittle/brittle-ductile-transition/ductile, so that the BDT layer can successfully connect the brittle PP layer and ductile PP/POE layer. Thereby the material breaks by ductile fracture as a whole. In addition, the existence of the rigid PP layer can provide ductile PP/POE layer with rigidity when the force propagates perpendicular to layers in turn. So the rigidity of material keeps very well, which is helpful to obtain material with balanced toughness and rigidity. However, as shown in Fig.11 (b), the formation of the BDT layer does not play the role of a bridge connecting the brittle PP layer and ductile PP/POE layer when the alternating multilayered material was impacted through z direction. Since the force propagates along the brittle PP layer, BDT layer and ductile PP/POE layer, respectively. So the material breaks by brittle fracture as a whole, and the rigidity keeps not very well.

On the other hand, previous study indicates that the conventional blend with 20 wt% POE is brittle. So for conventional blends (C-20) impacted through either y direction or z direction there is only brittle

fracture mechanism due to the absence of the alternating multilayered microstructure (seen in Fig.12).

#### **4 CONCLUSIONS**

PP and PP/POE alternating multilayered materials were prepared using multilayered co-extrusion technology. Alternating multilayered materials became ductile at -40 °C at a lower POE content about 15 wt% due to the multilayered microstructure with alternating brittle PP layer and ductile PP/POE layer, while conventional blends with the same content of POE were brittle. The notched impact strength through y direction of alternating multilayered materials with 18 wt% POE at -40 °C was greatly improved compared with that of conventional blends with the same POE content. At the same time, the flexural modulus, flexural strength of alternating multilayered materials also kept very well. The great enhancement of toughness and balanced rigidity can be attributed to the transition layer, formed at the interlayer interface, which plays the role of BDT layer during the impact process. This work provides us not only a deep insight into understanding elastomer toughening mechanism but also a new train of thought for toughening PP, which can greatly broaden the applied range of PP as high-performance structural materials with balanced mechanical properties.

#### **ACKNOWLEDGEMENTS**

Financial supports of the National Natural Science Foundation of

China (51273132, 51227802 and 51121001) and Program for New Century Excellent Talents in University (NCET-13-0392) are gratefully acknowledged.

## REFERENCES

- [1] Van der Wal A, Mulder J J, Oderkerk J, Gaymans RJ. *Polymer* 1998; 39: 6781.
- [2] Wu, S. *Polym Eng Sci* 1990; 30: 753.
- [3] Yang D, Zhang B, Yang Y, Fang Z, Sun G. *Polym Eng Sci* 1984; 24: 612.
- [4] Jang BZ, Uhlmann DR, Vander Sande J B. *J Appl Polym Sci* 1984; 29:4377.
- [5] Wu, S. *Polymer* 1985; 26: 1855.
- [6] Goizuetam G, Chiba T, Inoue T. *Polymer* 1992; 33: 886.
- [7] Phadke AA, De SK. *Polym Eng Sci* 1986; 26: 1079.
- [8] Wong, SC, Mai TW. *Polymer* 1999; 40: 1553.
- [9] Jang, BZ, Uhlmann, D R, Vander Sande, J B. *Polym Eng Sci* 1985; 25: 643.
- [10] Pukanszky B, Fortelny I, Kovar J, Tudos F. *Plast Rubber Compos Process Appl* 1991; 15: 31.
- [11] Van der Wal A, Gaymans RJ. *Polymer* 1999; 40: 6067.
- [12] Liu ZH, Zhang XD, Zhu XG, Qi ZN, Wang Fs. *Polymer* 1997; 38: 5267.

- [13] Van der Wal A, Nijhof R, Gaymans RJ. *Polymer* 1999; 40: 6031.
- [14] Jancar J, Dibenedetto AT. *J Mater Sci* 1994; 29: 4651.
- [15] Li LP, Yin B, Yang MB. *Polymer* 2012; 53: 3043-3051.
- [16] Masami O, Yoshihiro S. *Polymer* 1993; 23(34): 4868-4873.
- [17] Gao XL, Qu C, Zhang Q, Peng Y, Fu Q. *Macromol Mater Eng* 2004; 1(289): 41-48.
- [18] Z Li, S Guo, W Song, B Hou. *J Mater Sci* 2003; 38: 1793-1802.
- [19] Yin B, Li LP, Yang MB. *Polymer* 2013; 54: 1938-1947.
- [20] Geng CZ, Su JJ, Han SJ, Wang K, Fu Q. *Polymer* 2013; 54: 3392-340.
- [21] Deepak S, Pralay M, Emmanuel PG. *Adv. Mater.* 2004, 16, No. 14, July 19.
- [22] Qi D, Wang XF, Fan ZQ. *Polymer* 2007; 48: 5905-5916.
- [23] Xu HJ, Zhang YQ, Wang ZG. *Polym. Chem* 2013; 4: 3028-3038.
- [24] Yang H, Fu Q. *Polymer* 2006; 47: 2106-2115.
- [25] Zhang YQ, Xu HJ, Yang JJ, Wang ZG. *J. Phys. Chem. C* 2013: 117: 5882-5893.
- [26] Zhang YQ, Wang ZK, Jiang F, Wang ZG. *Soft Matter* 2013; 9(24): 5771 – 5778.
- [27] Zhang YQ, Fang HG, Wang ZK, Wang ZG. *Cryst.Eng.Comm* 2014; 16: 1026-1037.
- [28] Mohit Gupta, Lin YJ, Taneisha Deans, David A. Schiraldi.

- Macromolecules 2010; 43: 4230-4239.
- [29] Mueller CD, Nazarenko S, Ebeling T, Schuman TL, Hiltner A, Baer E. Polym Eng Sci 1997; 37: 355.
- [30] Tabatabaei, S. H.; Carreau, P. J.; Aji, A. J. Membr. Sci 2008, 325, 772.
- [31] Bai SL, Wang GT, Jean-Marie Hiver, Christian G' Sell. Polymer 2004; 45: 3063-3071.
- [32] Youn SL, Lee WK, Cho SG, Ha CS. J. Anal. Appl. Pyrolysis 78 (2007) 85-94.
- [33] Ren YZ, Masahiko S, Toshio N, Kimihiro M. et.al. J. Phys. Chem. B 1999, 103, 6475-6483.
- [34] D Quemada. Rheol Acta 1977, 16: 82-94.
- [35] Liu GY, Qiu GX. Polym Bull 2013; 70: 849-857.
- [36] Yang JH, Zhang Y, Zhang YX. Polymer 2003; 44: 5047-5052.

Table 1 Sample code, total sheet thickness, nominal layer thickness, total POE content in alternating multilayered materials and conventional blends

Sample code	Total sheet thickness (um)	Nominal PP layer thickness ( $\mu\text{m}$ )	Nominal PP/POE layer thickness ( $\mu\text{m}$ )	POE content (wt%)
C-0	1700	—	—	0
C-10	1700	—	—	10
C-20	1800	—	—	20
C-30	1700	—	—	30
AM-4	1700	16.7	10.0	3.98
AM-6	1700	10.5	16.0	6.2
AM-7	1700	8.4	18.1	7.1
AM-19	1700	14.8	11.9	8.67
AM-12	1800	10.8	17.4	11.85
AM-14	1700	6.8	19.8	13.9
AM-15	1700	14.1	12.4	15.4
AM-17	1700	11.3	15.2	16.77
AM-18	1800	10.8	18.2	18.16

a) POE content in PP/POE layer in AM-4, AM-6, AM-7 is 10wt%; in AM-9, AM-12, AM-14 is 20 wt%; in AM-15, AM-17, AM-18 is 30wt%.

Table 2 Orientation function (f) at 973 cm<sup>-1</sup> and 720 cm<sup>-1</sup>, peak area at 973 cm<sup>-1</sup> and 720 cm<sup>-1</sup>, peak area ratio between 973 cm<sup>-1</sup> and 720 cm<sup>-1</sup> in conventional blends and alternating multilayered materials

sample	f (973cm <sup>-1</sup> )	f (720cm <sup>-1</sup> )	Peak area (973 cm <sup>-1</sup> )	Peak area (720 cm <sup>-1</sup> )	Peak area ratio (720/973)	
Neat PP	0.421±0.018	—	1.386±0.013	0	0	
C-20	0.301±0.006	0.187±0.013	1.159±0.002	0.260±0.007	0.224	
AM-18	PP layer	0.387±0.010	—	1.353±0.011	0	0
	BDT layer	0.298±0.011	0.135±0.011	0.745±0.032	0.345±0.023	0.463
	PP/POE layer	0.267±0.008	0.108±0.011	0.610±0.009	0.387±0.015	0.634

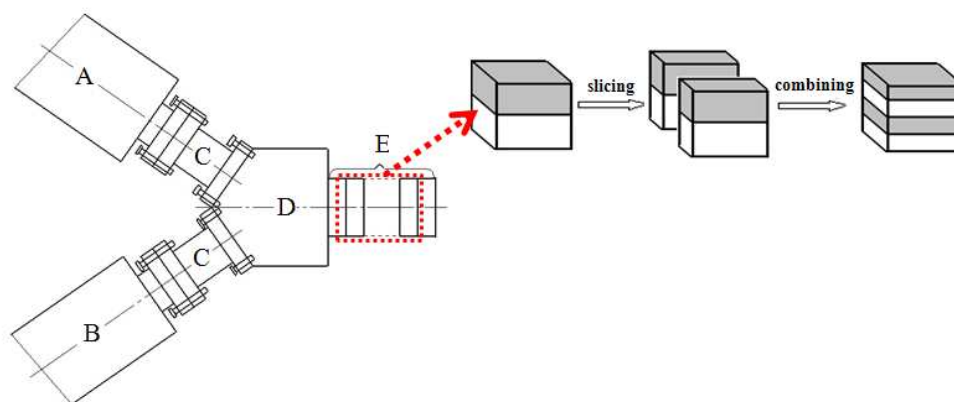


Figure 1 Sketch of multilayered co-extrusion technology: A, B-single screw extruder; C-connector; D-co-extrusion block; E-layer multiplying element (LME).

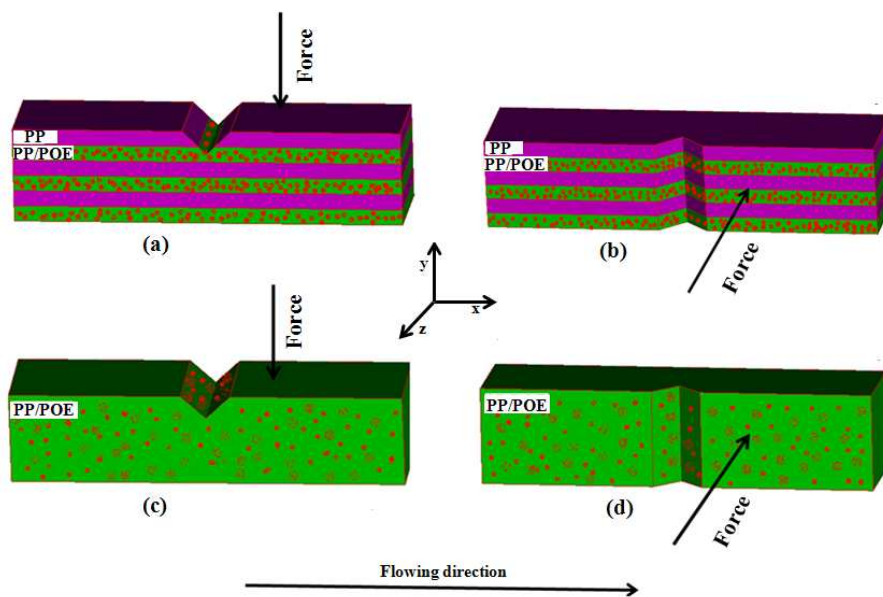


Figure 2 The schematic representation of impact test through different directions of alternating multilayered materials and conventional blends:(a) and (b) are alternating multilayered materials; (c) and (d) are conventional blends.

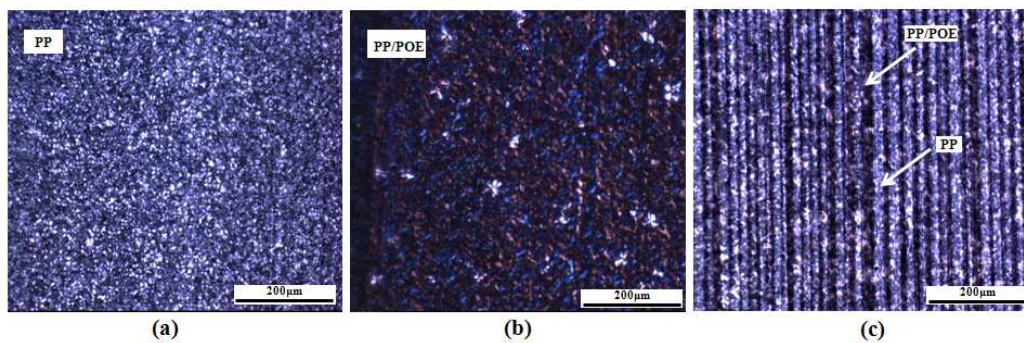


Figure 3 POM images of neat PP (a), conventional blend (b) and alternating multilayered material (c).

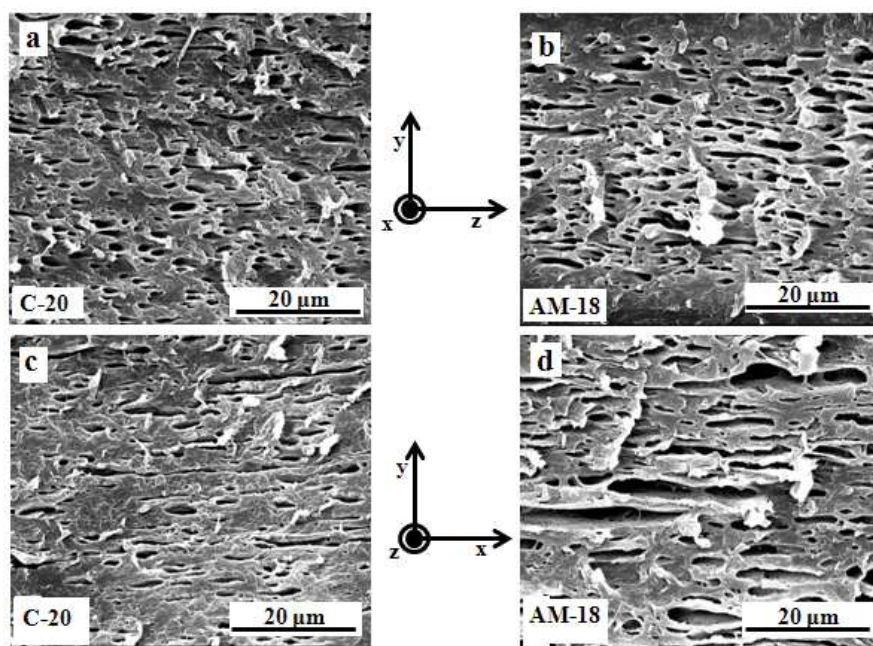


Figure 4 SEM images of heptanes etched surfaces before the impact of conventional blends and alternating multilayered materials: a and b are along y direction; c and d are along x direction.

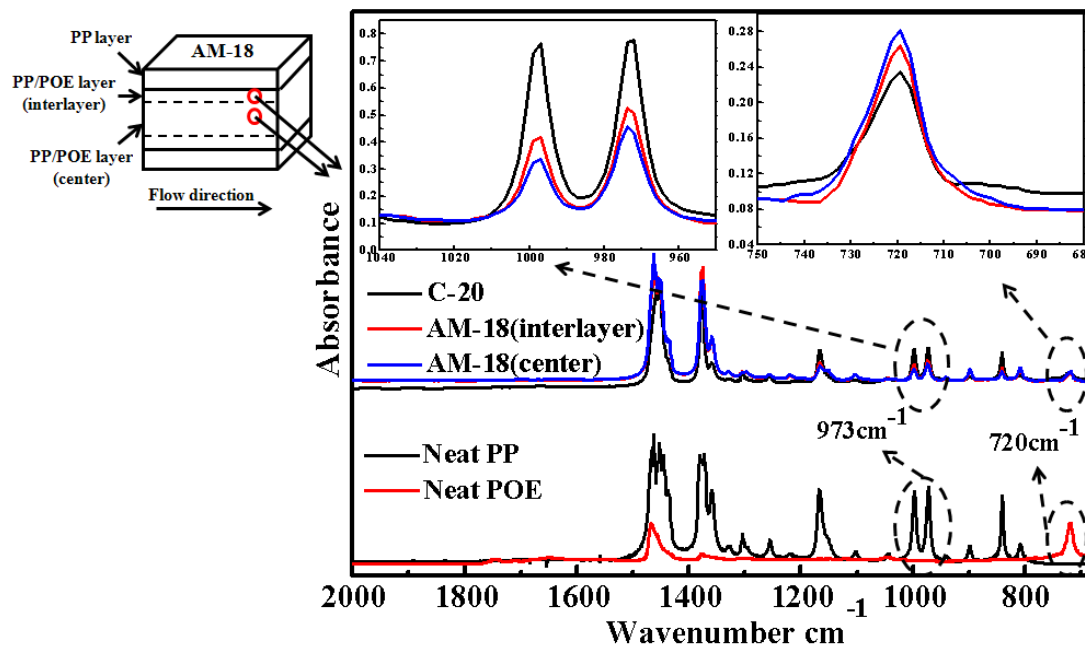


Figure 5 FTIR spectra absorbance of neat PP, neat POE, conventional blend (C-20), the interlayer in the PP/POE layer of alternating multilayered material (AM-18) and the PP/POE center layer.

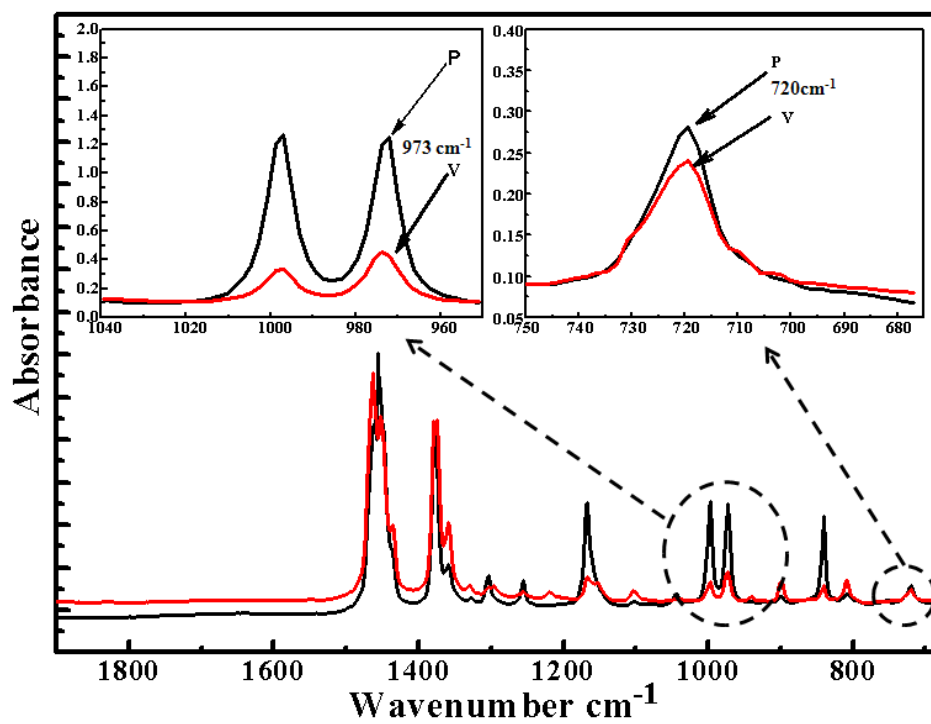


Figure 6 A typical part of FTIR spectra absorbance in the parallel and vertical direction for PP/POE blends.

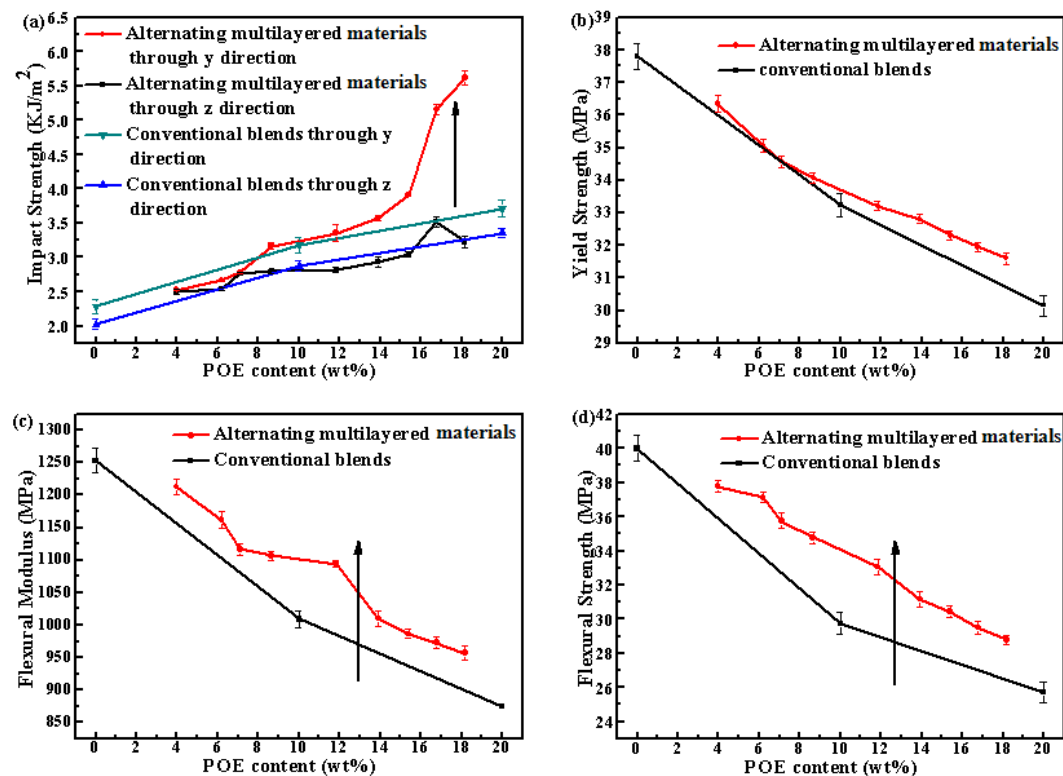


Figure 7 Mechanical properties of alternating multilayered materials and conventional blends via POE content (a): notched Izod impact strength at  $-40\text{ }^{\circ}\text{C}$  through different directions; (b): tensile yield strength; (c): flexural modulus; (d): flexural strength.

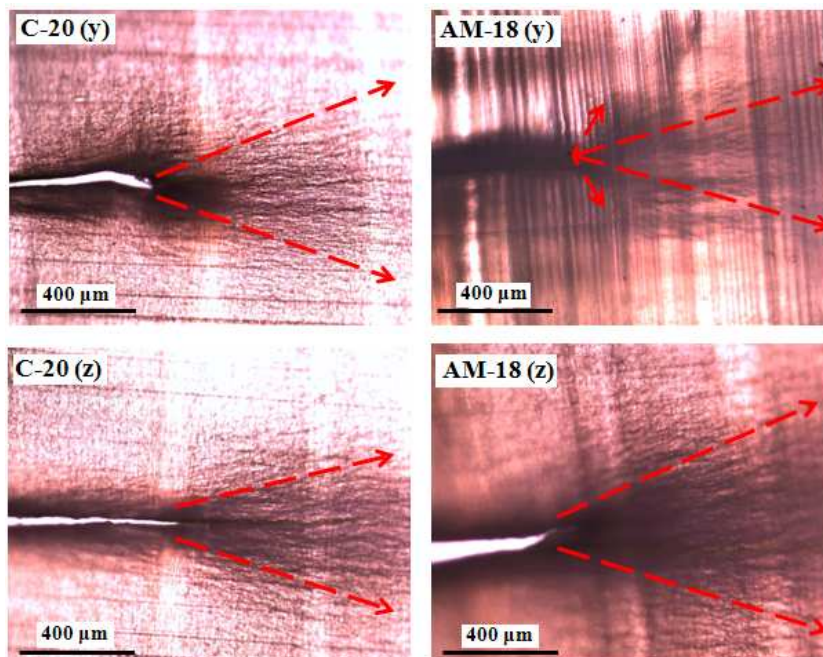


Figure 8 Initiation and propagation patterns of crack and craze of conventional blends and alternating multilayered materials after the part-impact test performed through y and z direction.

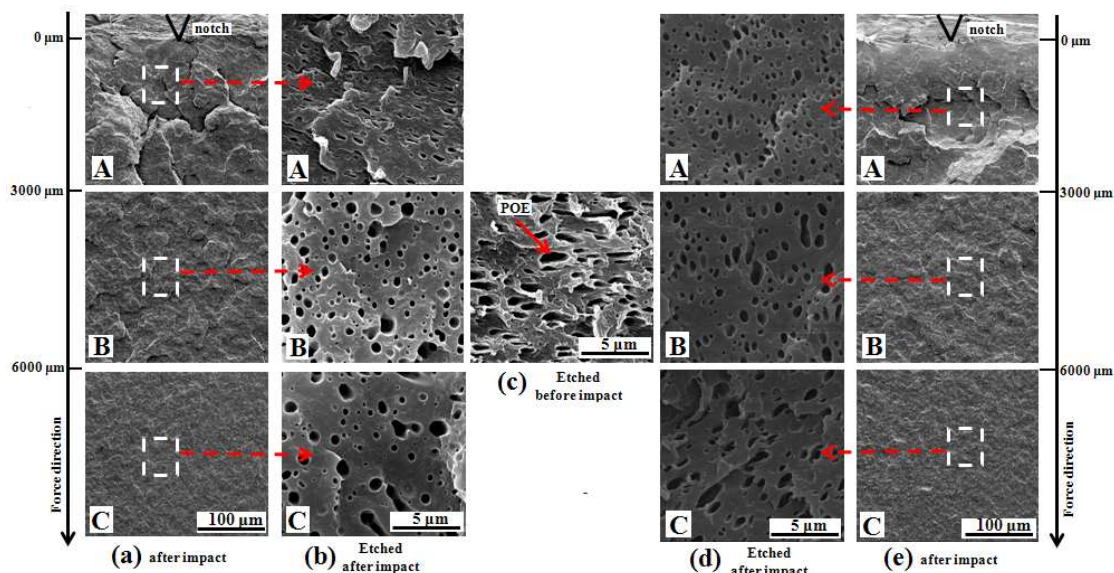


Figure 9 SEM images of impact fracture surface of conventional blend (a and e); heptane etched impact fracture surfaces (b and d); heptanes etched surface before the impact. (a) and (b) were the same sample impacted through y direction, (d) and (e) were the same sample impacted through z direction.

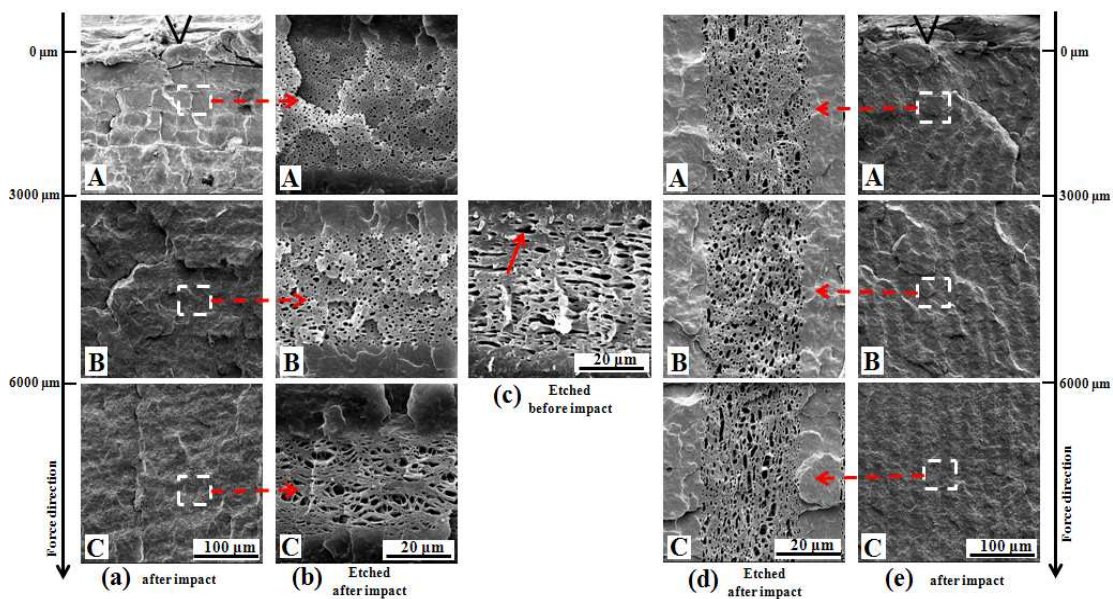


Figure 10 SEM images of impact fracture surface of alternating multilayered materials (a and e); heptane etched impact fracture surfaces (b and d); heptanes etched surface before the impact. (a) and (b) were the same sample impacted through y direction, (d) and (e) were the same sample impacted through z direction.

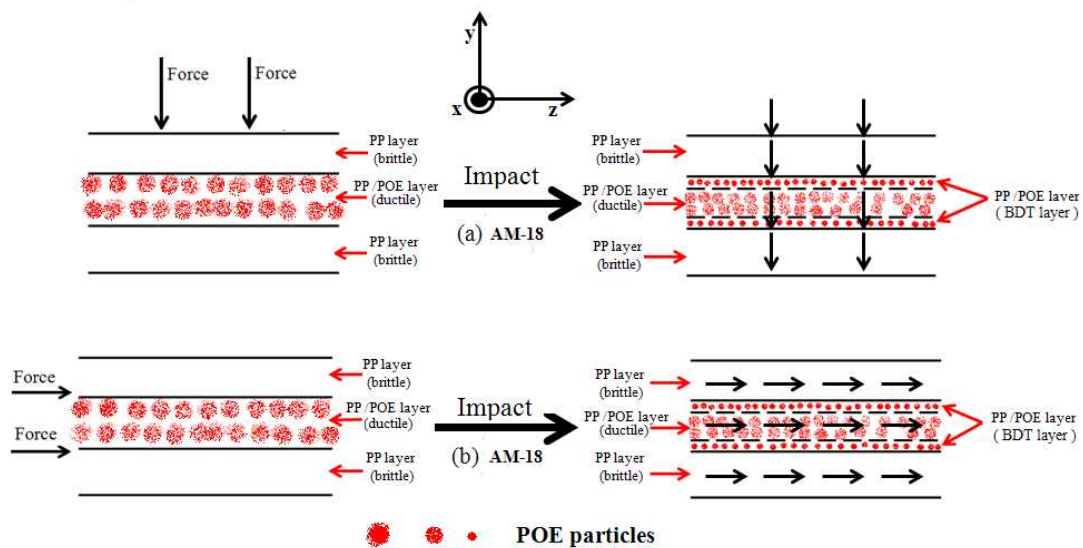


Figure 11 The schematic representation of toughening mechanism of alternating multilayered materials: (a) is impacted through y direction; (b) is impacted through z direction.

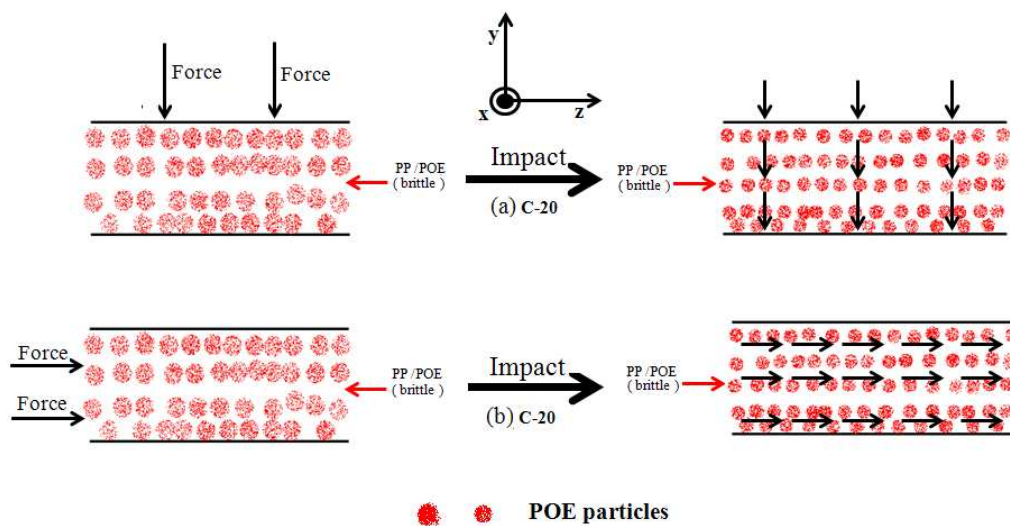
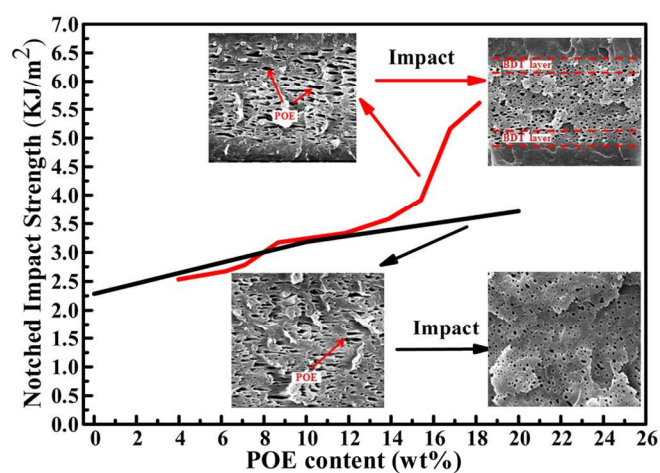


Figure 12 The schematic representation of toughening mechanism for conventional blends: (a) is impacted through y direction; (b) is impacted through z direction.



PP and PP/POE alternating multilayered material with unique macro and micro-morphologies can be fabricated through multilayered co-extrusion technology. During the impact process, BDT layer was formed at the interlayer interface between PP layer and PP/POE layer, which can successfully connect the brittle layer and ductile layer when the force was loaded perpendicular to layers. As a result, the notched impact strength at -40 °C , perpendicular to layers of alternating multilayered material, was greatly improved compared with that of conventional blend.